

Chemical Product and Process Modeling

Volume 2, Issue 2

2007

Article 11

PAPERS FROM CHEMECA 2006

Numerical Simulation of Electrolyte Two-Phase Flow Induced by Anode Bubbles in an Aluminum Reduction Cell

Naijun Zhou, *Central South University, Changsha, P.R.China*

Yuqing Xue, *Henan University of Science and Technology, Luoyang, P. R. China*

John J J Chen, *Auckland University, Auckland, New Zealand*

Mark.P. Taylor, *Auckland University, Auckland, New Zealand*

Recommended Citation:

Zhou, Naijun; Xue, Yuqing; Chen, John J J; and Taylor, Mark.P. (2007) "Numerical Simulation of Electrolyte Two-Phase Flow Induced by Anode Bubbles in an Aluminum Reduction Cell," *Chemical Product and Process Modeling*: Vol. 2: Iss. 2, Article 11.

DOI: 10.2202/1934-2659.1074

Available at: <http://www.bepress.com/cppm/vol2/iss2/11>

©2007 Berkeley Electronic Press. All rights reserved.

Numerical Simulation of Electrolyte Two-Phase Flow Induced by Anode Bubbles in an Aluminum Reduction Cell

Naijun Zhou, Yuqing Xue, John J J Chen, and Mark.P. Taylor

Abstract

In the production process of aluminium reduction cells, the anode bubble laden layer has several important influences on the performance of the aluminium reduction cells. Especially for a "drained cathode cell", without the agitating of movement of the melted metal, the bath flow field could be more important. In this paper, the electrolyte two-phase flow fields were studied by using numerically simulation method based on a two-phase turbulence model combining the $k - \epsilon$ model and the Discrete Random Walk model. The results show that: the motion of the bubbles mostly exists within a thin layer under the anode, which results in inducing local electrolyte to flow around the anode in various circulation flows; the flow field in the anode-cathode space can be divided into three regions with different characters; the results also show the Driving action of bubbles is closely related to the current density, inclination of anode and the anode-cathode distance. In general, the increasing in the current density increases the electrolyte velocity and the turbulent kinetic energy. The decrease in ACD significantly enhances the uniformity of the electrolyte flow field in the anode-cathode space. The increase in anode inclination angle increases the velocity of the electrolyte in the anode-cathode space, which would be beneficial to improving the diffusion and dissolution of the alumina and reducing the resistance between the anode and cathode.

KEYWORDS: aluminium reduction cell, anode bubbles, electrolyte flow, numerical simulation

1. INTRODUCTION

The anode bubble laden layer has several important influences on the performance of the aluminium reduction cells. The bubble layer will increase the bath resistance and the voltage drop of the cell, and promote the bath flow, etc.(Richards *et al*,2003). The flow field developed has a crucial effect on the dissolution and distribution of the alumina feed (Thonstad & Olsen, 2001).

Because of the corrosive nature and high temperature(~960□) of the electrolyte, it is either too costly or impossible to obtain information directly from the bath flow field(Dias & De Moura, 2005). Room-temperature analogy experiments are often used for studying the impacts of anode bubbles on the bath flow, and many researchers have reported their finding(Such as Fortin *et al*,1984; Chesonis *et al*,1990; Chen *et al*,1996; Poncsák *et al*, 1999; Alexandre *et al*,2005; Kiss *et al*, 2005).

However, there are discrepancies with the conclusions drawn by the various researchers. For example, Chesonis & Lacamera(1990) considered that the anode bubbles play the same role as the electromagnetic forces in promoting the bath flow. However others considered that the bubbles' role is more important (Purdie *et al*, 1993). There are also variations in the maximum velocities in the bath reported (Solheim *et al*,1989; Purdie *et al*,1993; Langon *et al*,1990).

In the other hand, Due to the development of suitable inert anode materials, a new cell design known as "drained cell", which has a sloped cathode and anode, has provided some advancement in recent years (Brown *et al*,1998). The inclined anodes result in increased bubble velocities and reduced bubble coverage under the anodes. The part played by bubbles in this inclined-anode situation is therefore different compared to the case of the horizontal anodes. It is therefore important to study the bath flow field caused by anode bubbles. However, up to now, systemic research work is still limited.

There are several advantages in studying the bath flow field using numerical simulation. For example, it is convenient to get its effects while any parameter involved varies so that the experiment expenses can be saved to some extent. Furthermore, the results obtained may be easily visualized. Therefore the numerical simulation method has been applied extensively in recent years. In this paper we apply the method to analyze firstly the electrolyte two-phase flow field under and around a single anode, and then we investigate the possible effects when some parameters are changed.

2. PHYSICAL MODEL

Because of the complexity of the bath flow fields, the following assumptions are made:

- The movement and influence of any undissolved alumina particles existing in the bath is ignored;
- The bath flow field is incompressible; and only the steady-state situation is simulated;
- The bath is isothermal, and any effect of the temperature gradient on the bath movement is ignored;
- The electromagnetic effect is not considered (Actually, electromagnetic field has

important impact on the electrolyte flow field. However it is related to the frame of the bus bar and location of the anode in the reduction cell. The authors have analysed it in another paper (Zhou *et al.*,2006). As we emphasize on study of the flow field structure around an anode, to adopt the assumption will be convenient);

- The bath flow field is turbulent;
- There is no chemical reaction between the anode bubbles and the bath and the bubbles are spherical in shape with a diameter of 5mm (Suppose the dimension to be the thickness of bubble layer (Zoric & Solheim,2000));
- The break and coalescence of bubbles are ignored.

3. COMPUTATION MODEL AND PARAMETERS

As the anode gas can not be dissolved in the electrolyte, the flow of the anode gas and electrolyte are layered two-phase turbulent flow. Where, the electrolyte is treated as continuous phase, and we use the standard $k-\varepsilon$ two-equation models to close the turbulence movement equations. Here, $k \equiv \overline{u_i' u_i'}/2$ is the turbulent kinetic energy and $\varepsilon \equiv \nu \overline{\partial u_i'/\partial x_j (\partial u_i'/\partial x_j + \partial u_j'/\partial x_i)}$ is the turbulence dissipation rate. In this paper, the bubbles are treated as particles to be dispersed within the continuous phase, and the Discrete Random Walk model is used for solving their velocities and tracks. The authors used the software FLUENT to solve the problem. The relevant coupled equations can be found in the user manual.

The computational zone is the domain under and around a single anode as shown in Figure 1. The top boundary of this domain is bath top surface, and the bottom boundary is the bath-carbon cathode interface. The other boundaries are the cell sidewall, the mid-position of the centre channel, and the mid-section of the inter-anode gap on either side of the anode under consideration.

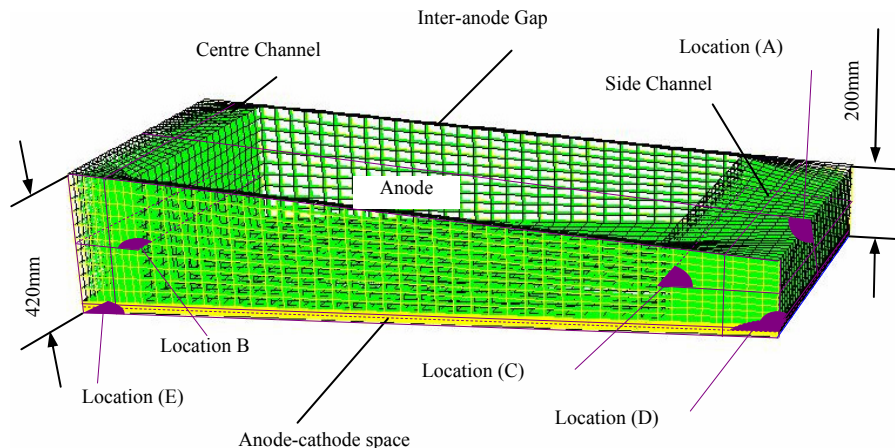


Figure 1. Analytic domain and grids

The Locations as segregated in Figure 1 include:

- (A) Vertical plane at the mid-point of the anode under consideration;
- (B) The horizontal plane at the one-half height of the centre channel;
- (C) The horizontal plane at one-half height in the side channel;
- (D) The horizontal plane below the back surface of the anode at the first grids layer;
- (E) The bottom plane of the bath at the first grids layer from the cathode.

The various parameters in the analytic zone are shown in Table 1.

Table 1. Parameters of the analytic zone

Length of anode /cm	150
Width of anode /cm	70
Distance between anode and the vertical plane at the mid-point of centre channel /cm	20
Distance between anode and the vertical plane at the mid-point of inter-anode gap /cm	2
Side channel /cm	30
ACD /cm	3
Anode slope /°	6
Current density /A · cm ⁻²	0.78
Temperature of bath /°C	960

Further simplification of the analytic zone is made by assuming that all the solid surfaces are smooth, the influence on the bath flow field due to the shape of the cell sidewall is ignored. Structured grids are used for the mesh employed in the domain, with a denser mesh in the domain of the anode-cathode space. There are a total of 41443 nodes and 37056 elements in the analytic domain (as shown in Figure.1).

There is no entrance or outlet boundary for the electrolyte, so all of the exterior of surface in the analytic domain are “wall” or “symmetrical plan”. All the “walls” are considered to be non-slip plane. The back surface of the anode is defined as the entrance boundary, and the top surface of bath is defined as the outlet boundary for anode bubbles.

The flow rate of the anode bubbles is calculated according to Fortin *et al* (1984) and the result is $0.0007\text{kg} \cdot \text{s}^{-1}$ for a current density of $0.78 \text{ A} \cdot \text{cm}^{-2}$.

The physical properties of the electrolyte and the anode gas are obtained from Solheim *et al* (1989).

4. RESULTS AND DISCUSSION

The computed results of bath flow field are shown in Figure 2 to Figure 10, in which the isolines show the distribution of the turbulent kinetic energy per unit mass.

Figure 2 shows the flow field in the anode-cathode space. The region in which the velocities of bath exceed $10\text{cm} \cdot \text{s}^{-1}$ is mainly at the upper layer of the anode-cathode space, and the side channel. The region in which the turbulent kinetic energy is bigger is mainly at the bottom of the side channel and the centre channel. The maximum and mean velocity in the bath is $24.4\text{cm} \cdot \text{s}^{-1}$ and $2.6\text{cm} \cdot \text{s}^{-1}$ respectively.

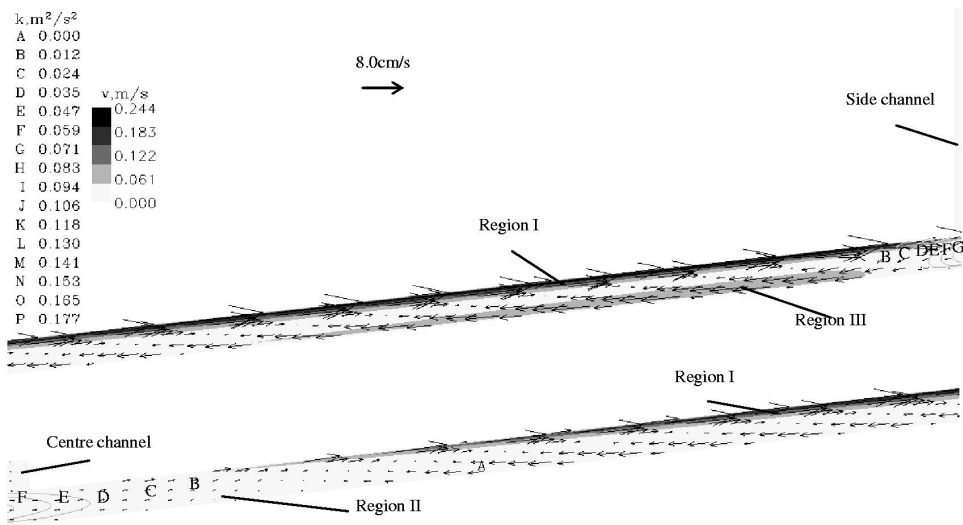


Figure 2. Flow field and turbulent kinetic energy in the anode-cathode space at Plane(A)

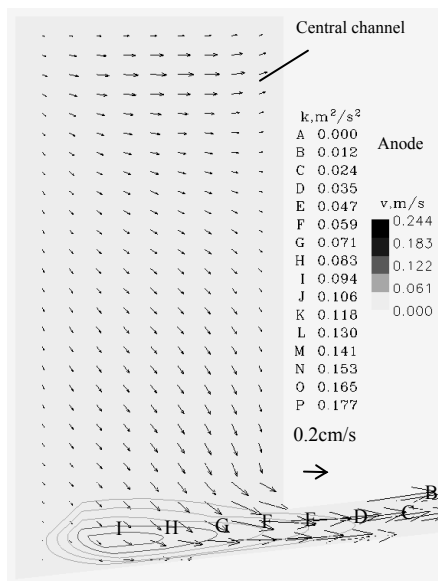


Figure 3. The velocity field and turbulent kinetic energy at centre channel at Plane (A)

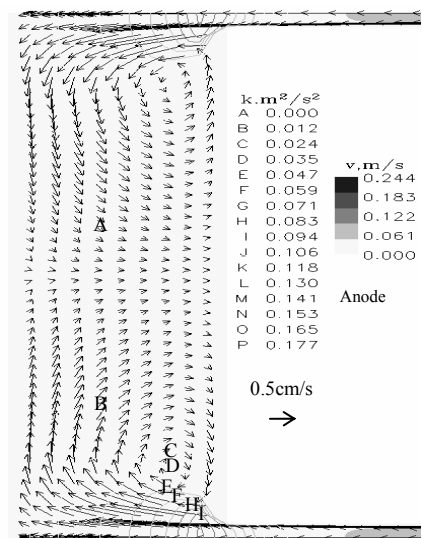


Figure 4. The flow field and kinetic energy at Plane (B)

Figure 3 and Figure 4 show the bath flow field in the centre channel, from which we can conclude that electrolyte in the centre channel flows mainly downwards and to the anode, before entering the anode-cathode space. The velocity in this area is very small and is less than $5\text{mm} \cdot \text{s}^{-1}$. The maximum turbulent kinetic energy is $0.094\text{m}^2 \cdot \text{s}^{-2}$.

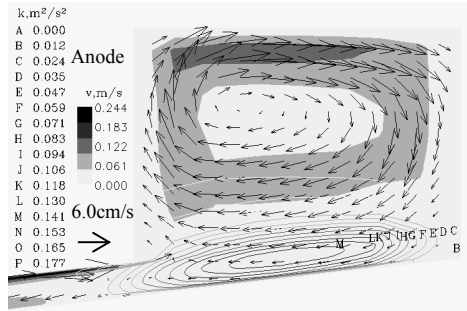


Figure 5. The flow field and turbulent kinetic energy in the side channel at Plane (A)

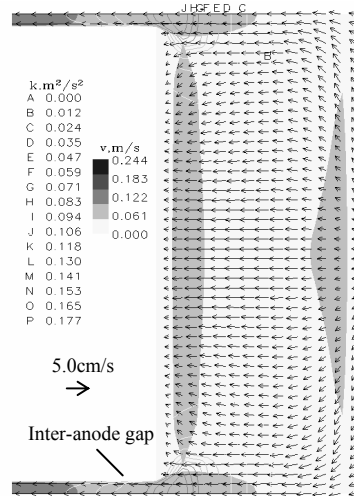


Figure 6. The flow field and turbulent kinetic energy at Plane (C)

Figure 5 and Figure 6 show the bath flow field in the side channel. The velocity field in this region resemble a whirlpool. In the region near the anode and the bath surface, the electrolyte flow velocity is the highest.

According to above results, in the anode-cathode space, the movement of the bath can be divided into two layers and three regions (Figure 2 and Figure7). In the upper layer (Region I), the electrolyte movement follows the moving bubbles, and the velocity is growing during its movement. The lower layer can be divided into two regions (Region II and Region III). In Region II, the lower layer near centre channel, the electrolyte flow into the side channel in the same way as the bath in the upper layer, and the velocity is below $1\text{mm} \cdot \text{s}^{-1}$. In Region III, the lower layer near the side channel, and the maximum velocity is about $7\text{cm} \cdot \text{s}^{-1}$. The turbulent kinetic energy in the anode-cathode space is very small.

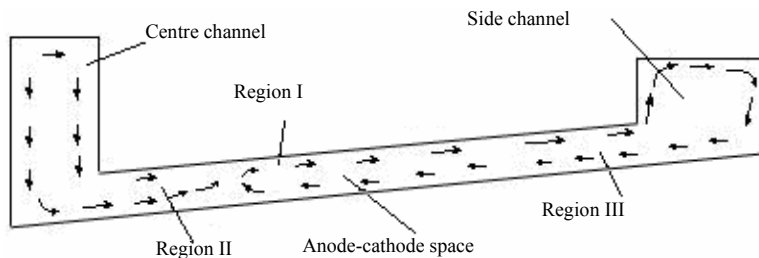


Figure 7. Schematic depiction of the bath flow field at Plane(A)

The electrolyte in the upper layer of the anode-cathode space flows primarily into the side channel. However, the flow of the electrolyte in the lower layer is more complex. It flows from the side channel towards the bottom of the anode, and some of the flow form spiral vortex or flow into the inter-anode gap. The detail velocity profile is shown in Figure 8. Generally, the velocity is small, and maximum value is below $8.5\text{cm} \cdot \text{s}^{-1}$.

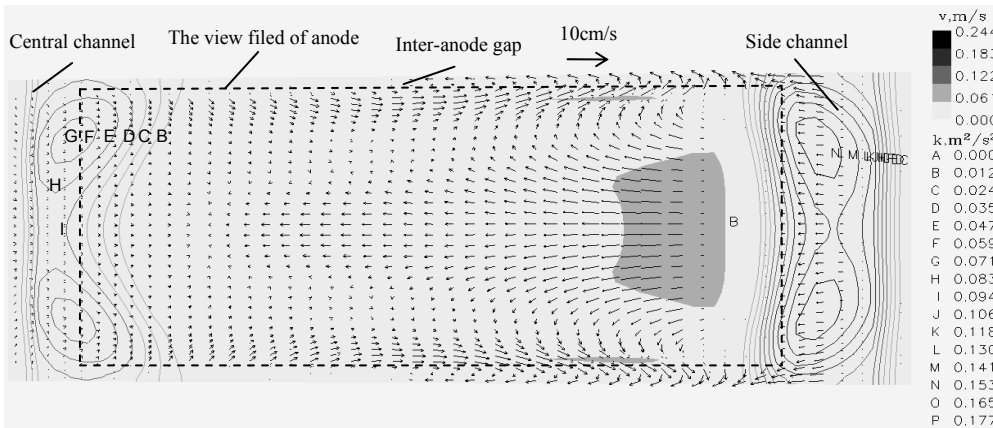


Figure 8. The flow field and turbulent kinetic energy at Plane(E)

Figure 9 is the bath flow profile in the inter-anode gap. From this figure we can see that the bath flow mostly from the side channel into the centre channel. However, some bath flow out the anode-cathode space and into the inter-anode gap near the side channel, while some other bath of flow out the inter-anode gap and into the anode-cathode space near the centre channel. The maximum velocity in this region reaches $18\text{cm} \cdot \text{s}^{-1}$, and the region near the surface of bath has relatively faster velocity.

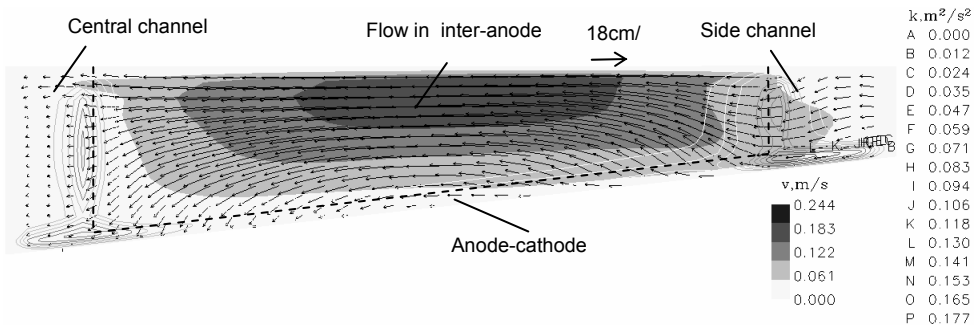


Figure 9. The flow field and turbulent kinetic energy at the inter-anode gap

Based on the analysis above, a schematic diagram is shown in Figure 10 to describe the overall bath flow field.

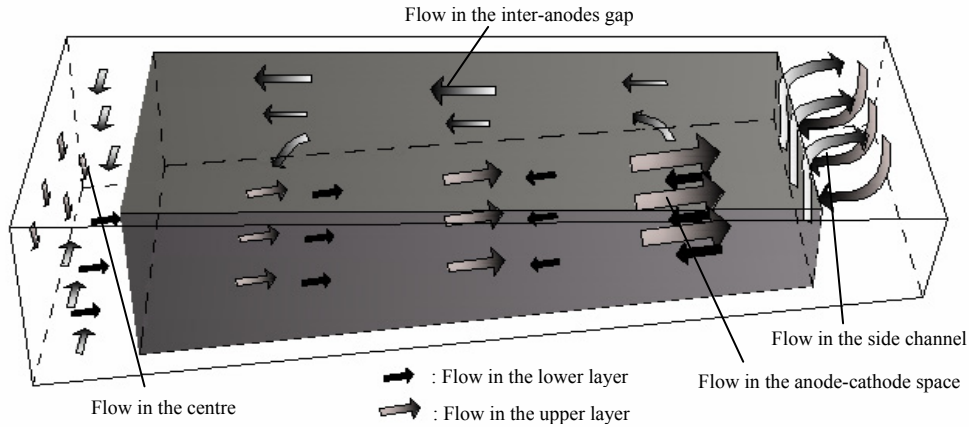


Figure 10. The sketch of electrolyte flow field at different regions around an anode

From Figure 10, it can be seen that the upper layer electrolyte in the anode-cathode space flows from the left to the right along the inclined channel with its being driven by anode bubbles, and with increasing velocity gradually. With the anode bubbles' releasing from the bath near the anode in the side channel, the electrolyte carried by the anode gas forms an approximately horizontal vortex in the side channel. Some electrolyte returns into the lower layer of the anode-cathode space. The other flows backwards the centre channel in the inter-anodes gap along two sides of the anode. However, there is a part of electrolyte to enter directly into the right inter-anodes gap from the anode-cathode space, which shows that some anode bubbles may release at these positions. At the same time, there is also a part of electrolyte to enter into the left anode-cathode space from the inter-anodes gap. The electrolyte coming from the inter-anodes gaps of the two sides comes together in the centre channel, and then flow downwards into the anode-cathode space. It should be noticed that there are different movement directions of the electrolyte from the left to the right in lower layer of the anode-cathode space.

It should be pointed out that the movement image of the electrolyte around an anode has been confirmed by a series of analogous room-temperature electrolysis experiments using bluestone solution which the authors undertook (Xue *et al*,2006).

5. EFFECTS OF CHANGING THE PARAMETERS

5.1 Effects of the current density

The first parameter to examine is the current density which changes the mass flow rate of the anode gas. It was found that the structure of the bath flow field remains unchanged, but the maximum and mean velocity are different as expected. The results are summarised in Table 2.

Table 2. The effect of the main parameters on the electrolyte flow field

Parameters	Results	Maximum velocity	Average velocity	Maximum turbulent kinetic energy	Average turbulent kinetic energy	Proportion of velocity over average value	Proportion of velocity over 10cm·s ⁻¹
		/cm·s ⁻¹	/cm·s ⁻¹	/m ² ·s ⁻²	/m ² ·s ⁻²	%	%
Current density /A · cm ⁻²	0.56	21.0	3.2	0.08	0.008	37.5	2.9
	0.78	24.4	3.6	0.18	0.019	37.4	5.7
	1.00	27.5	4.2	0.24	0.023	37.3	6.8
Anode-cathode distance (ACD) /cm	2	27.2	6.9	0.33	0.001	32.1	19.0
	3	24.4	3.6	0.18	0.019	37.4	5.7
	4	21.5	3.7	0.05	0.006	34.7	5.0
	5	21.1	3.5	0.04	0.006	26.7	4.5
Anode inclination angle /°	1.5	12.2	2.4	0.48	0.082	44.8	1.8
	3.0	20.0	3.9	0.22	0.025	42.6	7.0
	6.0	24.4	3.6	0.18	0.019	37.4	5.7
	8.0	25.3	5.0	0.08	0.009	28.7	6.8
	10.0	28.1	3.9	0.06	0.006	20.9	4.5

From Table 2, it may be concluded that the velocity and turbulent kinetic energy would increase with increasing current density. However, the magnitude of the area where velocity is higher than the mean velocity decreases slightly. As a result of increasing current density, the mass flow will increase. However, the bubbles only promote the bath within a finite layer. Thus, when the velocity of bath is increased, the unevenness of the flow field becomes more pronounced.

5.2 Effects of the ACD

The results for varying the anode-cathode distance (ACD) are also summarised in Table 2.

From the data listed in the Table, it may be deduced that the velocity and kinetic energy of the bath decreases when the ACD is increased, and the proportions of region in which the bath velocity exceeds the mean velocity and 10cm·s⁻¹ are gradually reduced. Thus, decreasing the ACD can improve the bubble-bath interaction.

It should be noticed that when the ACD is decreased to 2cm, the electrolyte flow pattern will change drastically. As the ACD is small, there is little back-flow layer at the bottom of the anode-cathode space, and Region III can hardly be found as shown in Figure 2 and Figure 7. At the same time, the velocity of the electrolyte is higher at the inter-anodes gaps.

5.3 Effects of the anode inclination angle

The results obtained by changing anode inclination angle are also shown in Table 2, which shows the changes in the velocity of the electrolyte and the turbulent kinetic energy.

Here, it should be pointed out that the total mass of the electrolyte is different when the inclination is changed, owing to the maximum depth being kept constant in calculation. Thus, with the angle increasing, though the maximum velocity increases, the average velocity does not always increase. In addition, when the inclination angle is 1.5°,

the maximum velocity in the centre channel is less than $0.05\text{cm}\cdot\text{s}^{-1}$, and the velocity in Region II is about $0.3\text{cm}\cdot\text{s}^{-1}$. Whereas the inclination angle is 10° , the maximum velocity in the centre channel is about $2.8\text{cm}\cdot\text{s}^{-1}$, and the velocity in Region II is about $3\text{cm}\cdot\text{s}^{-1}$, which is closer to the average velocity of the electrolyte. This shows that an increase in anode inclination angle helps to make the electrolyte flow in the anode-cathode space much more uniformly.

6. CONCLUSIONS

The movement and flow fields of the electrolyte induced by the anode gas bubbles around an anode have been modelled numerically. Based on the results obtained, the following conclusions can be drawn:

- The movement of the electrolyte induced by anode gas mainly is various circulation flows around the anode.
- The electrolyte's velocity and the kinetic energy distribution are not uniform, and the high velocity are located mainly in the region near down surface of the anode, the upper layer of the inter-anode gap, and the area near the end of the anode in the side channel.
- The electrolyte flow field in the anode-cathode space can be divided into two layers and three Regions. The velocity of the upper layer electrolyte in the anode-cathode space increases gradually along the direction of anode inclination.
- The current density, the anode-cathode distance (ACD) and the anode inclination angle all influence how the anode gas induces the flow of the electrolyte. Change in the current density merely changes the electrolyte velocity and the turbulent kinetic energy, but not to change uneven distribution of the electrolyte flow field. The decrease in ACD significantly enhances the uniformity of the electrolyte flow field in the anode-cathode space. The increase in anode inclination angle increases the velocity of the electrolyte in the anode-cathode space, which would be beneficial to improving the diffusion and dissolution of the alumina and reducing the resistance between the anode and cathode.

REFERENCES

- Alexandre P., Kiss L.I. and Poncsák S.; *Regimes of the Movement of Bubbles under the Anode in an Aluminium Electrolysis Cell*. Light Metals, **2005**: 565-570.
- Brown G.D., Hardie G.J. and Shaw E.W.; *TiB₂ Coated Aluminum Reduction Cells: Status and Future Direction of Coated in Comalco*. Proc. 6th Aust. Al Smelting Workshop, **1998**:499-508.
- Chen J. J. J., Shen X., Taylor M. P. and Welch, B.J.; *A Study of Bath Velocity Distribution in a 3-D Water Model*. Light Metals, **1996**: 343-350.
- Chesonis D. C. and Lacamera A. F.; *The Influence of Gas-driven Circulation on Alumina Distribution and Interface Motion in a Hall-Heroult Cell*. Light Metals, **1990**: 211-220.

Dias H.P. and De Moura R.R.; *The Use of Transversal Slot Anodes at Albras Smelter, Light Metals*, **2005**: 341-344.

Fortin S., Gerhardt M. and Gesing A. J.; *Physical Modelling of Bubble Behaviour and Release from Aluminium Reduction Cell Anodes*. *Light Metals*, **1984**: 721-741.

Kiss L.I., Poncsák S. and Antille J.; *Simulation of the Bubble Layer in Aluminium Electrolysis Cells*. *Light Metals*, **2005**: 559-564.

Langon B. and Peyneau J. M. ; *Current efficiency in modern point feeding industrial potlines*. *Light Metals* **1990**, 267-274.

Richards N., Gudbrandsen H., Rolseth S. and Thonstad J.; *Characterization of the Fluctuation in Anode Current Density and "Bubble Events" in Industrial Reduction Cells*. *Light Metals*, **2003**: 315-322.

Poncsák S., Kiss L. I. and Bui R. T.; *Mathematical Modelling of the Growth of Gas Bubbles under the Anode in the Aluminium Electrolysis Cells*. *CIM Light Metals*, **1999**: 57-72.

Purdie J.M., Bilek M., Taylor M.P., Zhang W.D., Welch B.J. and Chen J.J.J.; *Impact of Anode Gas Evolution on Electrolysis Flow and Mixing in Aluminum Electrowinning Cells*. *Light Metals*, **1993**: 355-360.

Solheim A., Johansen S.T., Rolseth S. and Thonstad J.; *Gas Driven Flow in Hall-Heroult Cells*. *Light Metals*, **1989**: 245-252.

Solheim A., Johansen S. T., Rolseth S. and Thonstad J.; *Gas induced bath circulation in aluminum reduction cells*. *Journal of Applied Electrochemistry*, **1989**, 19(5): 703~712.

Thonstad J. and Olsen E.; *Cell Operation and Metal Purity Challenges for the Use of Inert Anodes*. *JOM*, **2001**,53(5): 36-38.

Xue Y, Zhou N. and Bao S.; *Normal temperature analogue experiment of anode bubble's behavior in aluminum electrolysis cells*. *The Chinese Journal of Non-ferrous Metals(in Chinese)*, **2006**,16(10): 1823-1828.

Zhou N., Xia X. and Bao S.; *Effect of electromagnetic force and anode gas on electrolyte flow in aluminum electrolysis cell*. *Journal of central south university of technology*, **2006**, 13(5):496-500.

Zoric J., Solheim A.; *On Gas Bubble in Industrial Aluminum Cells with Prebaked Anodes and Their Influence on the Current Distribution*. *J. Applied Electrochemistry*, **2000**, 30: 787-794.